Selection-free non-viral method revealed highly efficient CRISPR-Cas9 genome editing of human pluripotent stem cells guided by cellular autophagy

Michelle Surma[1], Kavitha Anbarasu[1,2] and Arupratan Das[1,2,3,4,5,*]

[1]Department of Ophthalmology, Eugene and Marilyn Glick Eye Institute, Indiana University, Indianapolis, IN 46202, USA; [2]Department of Medical and Molecular Genetics, Indiana University, Indianapolis, IN 46202, USA; [3]Stark Neurosciences Research Institute, Indiana University, Indianapolis, IN 46202, USA; [4]Department of Biochemistry and Molecular Biology, Indiana University, Indianapolis, IN 46202, USA

[5]Lead Contact
[*]Correspondence: arupdas@iu.edu

SUMMARY

CRISPR-Cas9 mediated genome editing of human pluripotent stem cells (hPSCs) provides strong avenues for human disease modeling, drug discovery and cell replacement therapy. Genome editing of hPSCs is an extremely inefficient process and requires complex gene delivery and selection methods to improve edit efficiency which are not ideal for clinical applications. Here, we have shown a selection free simple lipofectamine based transfection method where a single plasmid encoding guide RNA (gRNA) and Cas9 selectively transfected hPSCs at the colony edges. Upon dissection and sequencing, the edge cells showed more than 30% edit frequency compared to the reported 3% rate under no selections. Increased cellular health of the edge cells as revealed by reduced autophagy gene-expressions is critical for such transfection pattern. Edge specific transfection was inhibited by blocking lysosomal activity which is essential for autophagy. Hence, our method provides robust scarless genome-editing of hPSCs which is ideal for translational research.

INTRODUCTION

Genome editing of hPSCs by CRISPR-Cas9 provides many unprecedented advantages, from introducing disease specific gene deletions to precise DNA base pair changes. Genome edited hPSCs are differentiated to the human cell of interest for disease modeling, drug screening, or cell replacement therapy, with potential use for personalized medicine (Saha and Jaenisch, 2009). Successful delivery of Cas9 gene and gRNA specific to the target gene is critical for gene editing in hPSCs. However, CRISPR-Cas9 mediated genome editing of hPSCs is an extremely inefficient process with success rate less than 3% (Yang et al., 2013). To increase genome-editing efficiency in hPSCs, several approaches have been taken including: stable integration of a drug selection marker into the genome (Lombardo et al., 2007), transient selection (Sluch et al., 2018; Steyer et al., 2018), fluorescence-activated cell sorting (FACS) (Ding et al., 2013) and more recently a combination of electroporation and viral transduction based methods (Martin et al., 2019). While these methods have improved genome editing efficiency, they also possess unwanted consequences, such as permanent gene alterations through integration of selection markers which could disrupt the local transcriptional regulation and will make hPSCs incompatible for clinical applications. FACS based single cell sorting to enrich Cas9 expressing cells increased edit efficiency to 6.0% in hPSCs but with very low cell survival rate (Byrne and Church, 2015; Yang et al., 2013). Viral gene delivery methods require special skill in producing virus particles, which is a lengthy process and not ideal for most laboratories. Antibiotic selection to enrich the transfected cells activates innate immunity and genetic changes which are not ideal for downstream translational

applications (Mignon et al., 2015; Vandermeulen et al., 2011). Thus, there is a critical need for developing a CRISPR-Cas9 mediated genome editing technique for hPSCs without the need for any antibiotic selection, FACS sorting or complex viral transduction-based methods.

To achieve this goal, here we first explored the differential transfection potential of stem cells within a hPSC colony and have identified that cells at the colony edges selectively got transfected due to increased cellular health compared to the cells at the center. Using a single plasmid containing gRNA/Cas9 and lipofectamine based transfection, we found very high Cas9 expression with more than 30% genome editing frequency through non-homologous end joining (NHEJ) at the edge cells compared to the center. This simple but highly efficient scarless genome editing technique of hPSCs is ideal for disease modeling research and clinical applications.

RESULTS

Cells at the hPSC colony edges are selectively transfected by plasmid DNA

We used a simple lipofectamine-based transfection to hPSCs which requires only mixing of the lipofectamine reagent and plasmid DNA containing Cas9/gRNA followed by addition to the cells. To identify if hPSC culture shows any cellular pattern for transfection which could be exploited to enrich the transfected cells, first we transfected H7 human embryonic stem cells (H7-hESCs) by CAG-mCherry plasmid at the single cell level or at

the colony stage which is formed by compacting several cells. Much to our surprise, we observed stem cells at the colony edge got selectively transfected but not cells the at colony center (Figure 1A), while single cell culture got transfected randomly with no such pattern (Figure 1B) as observed by the mCherry fluorescence. However, overall transfected cell population showed no difference between the single cell and colony stages when measured by flow cytometer (Figures 1C, 1D). To measure if stem cells at the colony center are not expressing mCherry and hence not transfected, we drew a line across the colony center through the edges and measured the fluorescence intensity profile on that line (Figure 1E). Indeed, we observed specific fluorescence intensity peaks on the line corresponding to the edges but not at the center (Figure 1F). This observation was further verified by measuring fluorescence intensity around the colony edges and centers which showed significantly high expression at the edge but not at the center cells (Figure 1G). To test if selective transfection of the colony edge cells is a cell type specific phenomenon, we transfected human H9-ESCs and induced pluripotent stem cell (EP1-iPSCs) (Bhise et al., 2013) colonies with CAG-mCherry plasmid. Indeed, we observed increased transfection of the peripheral cells for both the hPSC lines (Figure S1A, S1D). This observation was further verified by measuring fluorescence intensity profiles across the line through the colony center (Figure S1A, S1D) which showed specific intensity peaks at the colony edges but not at the center (Figure S1B, S1E). Similarly, fluorescence intensity measurements showed significantly high fluorescence at the edges compared to centers (Figure S1C, S1F). As hPSCs could be maintained in various media which could affect transfection efficiency, we tested the two most commonly used stem cell media mTeSR1 (mT) and mTeSRplus (mTp) for their effect on hPSC colony transfection

to further identify the optimum media for transfection. We found significantly higher transfection of H7-ESC colonies when cultured in the mT compared to the mTp media (Figure S2A, S2B) and maintained hPSCs in the mT for this study. However, cellular stemness marker expressions such as OCT4, NANOG, SSEA1, SSEA4, Alkaline Phosphatase (ALPL), SOX2, NOTCH1 and NESTIN did not alter between mT and mTp media (Figure S2C) suggesting stemness property of hPSCs was unaffected when cultured in either media. To test if selective transfection of the colony edge cells is specific to the lipofectamine based transfection, we transduced H7-ESC colonies with the lentivirus containing GFP vector. Interestingly, we observed stem cells throughout the colony got transduced as shown by GFP expression losing the morphological pattern (Figure S3). These data suggest lipofectamine based simple transfection of hPSC colonies selectively transfects edge cells, which could then be isolated to enhance CRISPR genome editing without the need of any viral transduction and antibiotic selection methods.

Autophagy driven increased cellular health of hPSC colony edges caused increased cell transfection.

To investigate the mechanism of selective transfection of hPSC colony edge cells, we asked if cells at the colony edges have more access to the nutrients from the media than the cells at the center, leading to improved cellular health and transfection. Cellular health could be measured by gene expression of the autophagy pathway genes as they get upregulated under stress (Kroemer et al., 2010). Activation of the autophagy pathway

genes help by removing damaged proteins and organelles under cellular stress (Anding and Baehrecke, 2017). Hence, we expect cells at the hPSC colony centers will have more autophagy gene expression than the edges. To measure this, we dissected out the H7-hESC cells from the colony edges and centers (Figure 2A) and measured gene expressions for a broad range of autophagy genes (Sha et al., 2018). Indeed, we found key autophagy genes such as ATG5, LC3B, GABARAP, GABARAPL1 and ATG13 are upregulated at the center compared to the edge cells (Figure 2B) suggesting improved cellular health of the edge cells. Of note, the dissected center portion of colony (Figure 2A) also contain small portion of edges as dissection of only center cells are extremely difficult and growing colonies very large leads to colony fusions losing edge populations and spontaneous differentiation (Chen et al., 2014). Next, we asked whether the difference in cellular health between colony edge and center affects hPSC stemness property. To test this, we measured stemness marker gene expressions between the edge and center cells of H7-hESC colonies and found no significant difference (Figure 2C), suggesting stem cells maintained their stemness property throughout the colony. If stem cells at the colony edges show increased health due to the greater exposure to nutrients leading to more transfection, we asked if creating new edges at the colony center would lead to selective transfection of stem cells at the newly formed edges. To test this, we scratched at the center of H7-hESC colonies to form new edges (Figure S4A) followed by transfection using CAG-mCherry plasmid. Indeed, we observed that cells at the newly formed edges at the former colony center got transfected as shown by the mCherry expression (Figure S4B). Of note, we also have seen some stem cell transfection inside these colony centers (Figure S4B), presumably due to the change in cellular contact upon

scratching through the middle of colonies, which is a mechanical perturbation. These suggest that stem cells at the colony centers maintained their stemness as well as the ability to get transfected upon exposure to new edges.

It has been shown that cells at the hPSC colony edges experience strong myosin II molecular motor mediated contractility of the actin cytoskeleton leading to enhanced contraction of extracellular matrix (ECM) (Närvä et al., 2017; Rosowski et al., 2015). We asked if increased actomyosin contractility at the hPSC colony edges are responsible for selective transfection of these cells. To test this, we inhibited actomyosin contractility by the very potent myosin II ATPase inhibitor blebbistatin (Das et al., 2016) followed by transfection of H7-hESC colonies using CAG-mCherry plasmid. Interestingly, we observed that under myosin II inhibition cells at the edge as well as at the colony center got transfected, losing the edge specific transfection pattern as shown by mCherry expression (Figure 3A). We further observed an overall higher percentage of transfection under myosin II inhibition as measured by flow cytometry (Figure 3B, 3C) which also agrees with the previously reported data (Yen et al., 2014). Myosin inhibition presumably reduced cell-cell contact, making cells more exposed to the transfection reagent and causing cell transfection throughout the colony. Actomyosin contractility leads to the formation of thick F-actin stress fibers within the cells (Tojkander et al., 2012) which we observed in the edge cells of H7-ESC colonies with F-actin stained by fluorescence conjugated phalloidin, indicated by arrows (Figure 3D). We found successful inhibition of actomyosin contractility by blebbistatin as stress fibers disappeared at the hPSC colony edge cells (Figure 3D). Our data showed cells at the hPSC colony centers are under

stress with increased autophagy gene expressions compared to the edges. We asked if inhibition of the autophagy pathway would increase cellular stress throughout the hPSC colony leading to the inhibition of edge specific cell transfection. To test this, we inhibited the autophagy pathway by using a lysosome inhibitor bafilomycin, followed by CAG-mCherry plasmid transfection. Indeed, we found loss of colony edge specific transfection (Figure 3A) with reduced overall transfection under autophagy inhibition (Figure 3B, 3C) but no loss of F-actin stress fibers at the edge cells was observed (Figure 3D). These data suggest increased cellular health but not the actomyosin contractility of the hPSC colony edge cells is responsible for the selective transfection of those cells.

Edge cells at the hPSC colonies showed very high efficiency CRISPR genome editing.

Finally, we asked if selective transfection of the hPSC colony edge cells could be exploited to have high-efficient CRISPR-Cas9 genome editing. To test this, we transfected H7-hESC colonies using lipofectamine and a plasmid encoding gRNA under U6 promoter and SpCas9-2A-GFP under CAG promoter (Figure 4A). 2A is a non-translatable sequence (Sharma et al., 2012) and after translation, SpCas9 and GFP remain separate without effecting the protein activity. We hypothesized selective transfection of the hPSC colony edge cells would lead to enhanced Cas9 expression in those cells. To test this, we transfected H7-hESC colonies with the above plasmid and dissected out colony edge and center as shown in Figure 4B and measured Cas9 expression in the respective populations. Indeed, we observed several fold increased

Cas9 expression in edge cells compared to the center (Figure 4C). This is very important as Cas9 delivery followed by gRNA-guided DNA double-strand break (DSB) leads to the insertion-deletions (INDELs) which is the rate-limiting step for obtaining high-frequency genome editing (Hendel et al., 2014, 2015).

Next, we cloned gRNA into the Cas9 vector (Figure 4A) for mutating hypoxanthine phosphoribosyltransferase 1 (HPRT1). Upon transfection of the H7-hESCs colonies with this plasmid, we observed selective transfection of the cells at the colony edge by GFP expression (Figure 4D) similar to the CAG-mCherry plasmid. gRNA targets a specific gene sequence which allows the Cas9 enzyme to bind and create DNA DSB which cells repair by NHEJ. NHEJ leads to INDELs causing gene mutations. These mutations could be detected by PCR amplifying the DNA sequence around the gRNA target site followed by sanger sequencing and TIDE analysis (Brinkman et al., 2014) of the sequencing data. Since we observed high Cas9 expression in the edge cells, we hypothesized this will lead to high INDEL frequency. Indeed, by TIDE analysis we observed ~38% of edge cells with mutations (62% at 0 INDEL corresponds to 38% mutation) for HPRT1-gene in comparison to the center cells (Figure 4E, F). This is a significant improvement from the reported 3% mutation rate of hPSCs under non-viral and selection free conditions (Yang et al., 2013). This is remarkable as for the first time it allowed us to identify cells from stem cell colonies with very high-frequency genome editing without the need for any viral transduction, FACS sorting or antibiotic selections.

DISCUSSION

Our work here demonstrated properties of hPSCs within a colony and how that could be used to achieve a selection and viral transduction free CRISPR-Cas9 genome editing technique with very high edit-frequency. This work will have three major impacts on the human disease modeling research; (1) the absence of any antibiotic selection marker will avoid integration of the marker gene and Cas9 into the hPSC genome avoiding unwanted scars or changes, (2) the simple lipofectamine reagent based transfection would allow us to use two or more plasmids with gRNAs targeted for different genes to have double or triple gene knock-out simultaneously, (3) this technique could also be used to create disease causing DNA base pair changes (point mutations) or correct mutations in the patient derived iPSCs by using Cas9 plasmid and single-stranded oligodeoxynucleotides (ssODNs) donor or donor vector. The lipofectamine-stem reagent is compatible for transfecting hPSCs with plasmids as well as ssODNs. Being able to seamlessly edit hPSCs would allow us to differentiate genome edited stem cells to the cell of interest and investigate the human disease mechanism, perform drug screening to identify cell protective agents and replace damaged cells with healthy cells in in-vivo models for cell replacement therapy. This will bring a paradigm shift in the understanding of genotype-phenotype relationship for a variety of human diseases.

Our data suggested selective transfection of the colony edge cells is due to improved cellular health as revealed by low autophagy gene expressions compared to the center cells (Figure 2). However, it is also possible that the edge cells are more exposed to the transfection reagents than the center leading to increased transfection. This notion could

238 be supported by our colony scratch experiment where cells at the new edge in the middle
239 of hPSC colonies got transfected (Figure S4). Our data (Figure 3C) as well as data from
240 another group (Yen et al., 2014) have shown inhibiting actomyosin contractility increased
241 hPSC colony transfection, which could be due to the reduced cell-cell contact within the
242 colony centers exposing cells more to the transfection reagents. Thus, selective
243 transfection of the hPSC colony edge cells could be due to the combination of increased
244 cellular health and more exposure to the transfection reagents.
245
246 **Limitations of Study**
247 This study reveals a very simple but high-efficient genome editing technique in hPSCs
248 with tremendous potential for a broad range of gene editing applications. As a next step,
249 this technique could be used for introducing point mutations in hPSCs or correcting
250 mutations in patient derived iPSCs. Our method here relies on the compact hPSC colony
251 formation to have the distinct edge and center cell population. hPSCs typically grow
252 forming these compact colonies; however if stem cells are grown in non-colony type
253 monolayer (NCM) (Chen et al., 2012) they will not have distinct edge and center cell
254 populations, and hence will limit this method application.
255
256 **ACKNOWLEDGEMENTS**
257
258 This work was supported by the grant from the NIH, United States (R00EY028223). We
259 thank Dr. Donald Zack for kindly providing the H7-hESC, H9-hESC and EP1-iPSC human

pluripotent stem cell lines and Drs. Jason Meyer, David Wallace and Timothy Corson for valuable discussions.

AUTHOR CONTRIBUTIONS

M.S. and A.D. designed the experiments, analyzed data and wrote manuscript; M.S. performed experiments and analyzed data with the help of K.A; A.D. conceived and supervised the project and revised the manuscript.

DECLARATION OF INTERESTS

The authors declare no competing interests

FIGURE LEGENDS

Figure 1: hESCs selectively got transfected at the colony edges but not at center. H7-hESCs after clump or single cell passage were transfected with CAG-mCherry (red fluorescence protein, RFP) plasmid and representative brightfield and RFP images were taken 24h after transfection. Shown are images of colony **(A)** and single cells **(B)**. **(C, D)** Transfected cells were dissociated by accutase and run through flow cytometer; shown are the distribution of the RFP-positive cells **(C)** and quantification for percentage of total RFP-positive cells **(D)** with 3 biological repeats for each condition. **(E-F)** Representative images of clump passaged colony 24h after transfection with CAG-mCherry plasmid **(E)**, line trace through the center of colony as shown in (E) shows fluorescence intensity peaks

at the edges **(F)** but not at the center. **(G)** Quantification of the fluorescence intensity of colony edges and centers from 58 colonies from 5 independent experiments. Error bars are SEM, Student's *t-test*, ***, $p < 0.0005$.

Figure 2: hPSCs at the colony edges are healthier with reduced expression of autophagy genes.

(A) H7-hESCs were cultured and colony edges and centers were dissected for qPCR. **(B, C)** qPCR analysis was done on the autophagy genes **(B)** and stemness marker genes **(C)**. ΔΔCt fold changes were measured relative to GAPDH and then to average ΔCt of center. Error bars are SEM, Student's *t-test*, *, p-value < 0.05, n=7-15.

Figure 3: Inhibiting autophagy but not actomyosin contractility decreases transfection efficiency.

(A) H7-hESC colonies were treated for 16h with blebbistatin or bafilomycin, then transfected with CAG-mCherry plasmid, shown are images 24h after transfection. **(B, C)** Single cell solutions were collected 24h after transfection and run through flow cytometer, shown are the distribution **(B)** and percentage of RFP-positive cells with-respect-to (w.r.t) control **(C)**. Error bars are SEM, One-way Anova with Dunnett's post hoc; **, p-value < 0.001, n=3. **(D)** Shown are representative confocal immunofluorescence images of F-actin labelled with Alexa Fluor 488 Phalloidin and nucleus labeled with DAPI of H7-hESCs treated for 24h with the indicated drugs. Arrows indicate normal actin stress fiber bundles, n=12.

Figure 4: Enhanced CRISPR-Cas9 genome editing at the hPSC colony edges.

(A) Map of plasmid (Addgene #79144) containing Cas9 and GFP cassettes. (**B, C)** H7-hESCs were transfected with the above plasmid, edges and centers were dissected after 24h as shown in **(B)**, and Cas9 expression was measured by qPCR **(C)**. Data presented as ΔCt fold change relative to GAPDH. Error bars are SEM, Student's *t-test*, ***, p-value < 0.0005, n=6-9. **(D-F)** HPRT1-gRNA was inserted into the Addgene plasmid and then transfected into H7-hESCs, shown are representative images after 24h of transfection **(D)**. Colony edges and centers were dissected and sequenced for HPRT1 mutation, shown are representative sequencing chromatographs **(E)** and INDEL distribution of edge cells compared to the center cells by TIDE analysis **(F)**, n=12.

STAR METHODS

Resource Availability

Lead Contact

Further information and requests for resources and reagents should be directed to Arupratan Das (arupdas@iu.edu)

Materials Availability

Stem cells and plasmids are available from the Lead Contact's laboratory upon request and completion of the Material Transfer Agreement.

Data and Code Availability

This study did not generate any code or dataset.

EXPERIMENTAL MODEL AND SUBJECT DETAILS:

H7-ESCs, H9-ESCs (WiCell, https://www.wicell.org/), and EP1-iPSCs were grown in mTeSR1 media (mT) or mTeSR-plus media (mTp) in 5%CO_2, 37^{o}C incubator on matrigel (MG) coated plates. To obtain hPSC colonies, cells were passaged by clump passaging using Gentle Cell Dissociation Reagent (GD) after reaching 80% confluency. GD was added to cells for 4 min at 37^{o}C, aspirated, then mT was used to resuspend colonies; cell suspension was mixed by pipetting 3-4 times to break up the colonies into small clumps and then seeded into new MG coated wells. Clump passaged colonies were cultured for an additional 2-3 days before experiments. For single cell passaging, cells were incubated with accutase for 10 min and then quenched with double volume of mT with 5 μM blebbistatin. These cells were pelleted by centrifuging at 150G for 5 min, and resuspended in media with blebbistatin, counted, and seeded at a density of 25,000/well of a 24-well plate.

METHOD DETAILS:

hPSC transfection

hPSCs were cultured as described above. The clump passaged colonies using GD were added to a larger volume of media and equally split into the wells of 24-well plates. Single cells after accutase passage were transfected 24h after seeding. GD cells were cultured for another 2-3 days until the colonies were established with distinct edges and centers with colony size around 1/10th the size of a 10x viewscreen at start of drug treatment or transfection. hPSC colonies were treated with 5 μM blebbistatin, 50 nM bafilomycin, or equivalent volume of DMSO in mT for 16h. Cell transfections were done by mixing 2 μl of lipofectamine stem (Invitrogen) and 600 ng of indicated plasmids in 50 μl optimem by vortex. 10 min after vortexing, this mixture was added to the cell culture and incubated for 24h. Images were taken by the EVOS fluorescence microscope (Thermo Fisher Scientific). Using ImageJ software, fluorescence intensity was quantified by drawing a 'donut' containing the colony edge, measured as the edge; the 'hole' of the donut was then measured as the center. Raw integrated density was divided by the total area to get the average intensity per area for both edge and center of each colony.

Flow Cytometry

For flow cytometry, cells were incubated in 40 μl accutase for 10 min, then quenched with 160 μl mT with 5 μM blebbistatin. This 200 μl cell suspension was transferred into a 96-well round-bottom plate and read on the Attune NxT Acoustic Focusing Flow Cytometer (Thermo) equipped with Attune Auto Sampler (Thermo). Gating was used first to separate live cells, then to separate RFP-positive from the live cell population using the Attune NxT Software. Data were exported to excel or prism for analysis and plotting. Three or more biological repeats were performed for each condition.

qPCR

hPSCs were grown in mT and clump passaged using GD. For mT and mTp comparison, H7-hESCs were cultured in the respective media in 6-well plates for more than 2 weeks before starting the experiment. Cells at ~80% confluency were passaged and seeded on 24-well MG coated plates for another 4-5 days until they reached ~70% confluency. Cells were incubated with 200 μl accutase for 10 min and resuspended in 400 μl mT with 5 μM blebbistation. Cells were then centrifuged at 150G for 5 min, media aspirated, and cell pellets stored at -20°C. For edge/center comparison, colony dissection was done two days after seeding using clump passaging. When colonies were grown to 1/4 of a 10x field size checked by EVOS, the edge was dissected out first, and then a slice from the center of the colony was collected as the center. Samples were collected into mT with 5 μM blebbistatin, with edges and centers from 10 distinct colonies collected into 1 biological replicate, with 3 biological replicates total for edge and center. Samples were then centrifuged, media aspirated, and cell pellets stored at -20°C until cDNA preparation. RNA extraction was done following the kit (Qiagen 74104) and 6 μl of RNA was used to prepare cDNA (abm G492). cDNA concentration was measured using Nanodrop 2000c (Thermo) and stored at -80°C. qPCR primers were designed as explained in Table S1. qPCR was performed using Brightgreen (MasterMix-LR, abm) and 100 ng total cDNA in a 20 μl reaction mixture using QuantStudio6 Flex RT PCR system (Applied Biosystems). GAPDH was used as a housekeeping gene in every plate to calculate the ΔCt values. The ΔΔCt was calculated with respect to the average ΔCt of colony center (edge vs. center) or mT (mT vs mTp).

gRNA Cloning

gRNA sequence targeting HPRT1 was obtained from Thermo Fisher (A32060), and then modified following the published protocol (Ran et al., 2013). gRNA was cloned after the U6 promoter sequence into a plasmid containing pCAG-SpCas9-GFP-U6-gRNA (Addgene #79144). 1 μg of plasmid was digested using 1 μl of Bbs1-HF in 1X cutsmart buffer in a total reaction volume of 50 μl. This was then run in 1% agarose gel, and gel extracted following the kit (Zymo D4007).

10 μM of sense and antisense gRNA oligos were added to 1X T4 DNA ligase reaction buffer with 0.5 μl of T4 Polynucleotide Kinase for a final volume of 10 μl and annealed in the thermocycler (37°C for 30 min, then 95°C for 5 min, and ramp down to 25°C at 5°C/min). The annealed gRNA was ligated into the gel extracted plasmid by adding 50 μg of the Bbs1-HF digested plasmid, 1 μl of annealed oligo duplex, and 5 μl of 2x quick ligation buffer for a final volume of 10 μl. 1 μl of quick ligase was then added and the reaction incubated at room temperature for 10 min. 2 μl of this plasmid was added to 50 μl of Top10 *E coli* and kept in ice for 5 min. The bacteria were then heat shocked to promote uptake of the plasmid at 42°C for 45 seconds before being placed back into ice for 2 min. 250 μl SOC media was added to the bacteria and incubated in a 37°C shaker for 1h before being spread onto LB-agar plates with Carbenicillin (50 μg/ml) and incubated overnight at 37°C. The next day, colonies were picked and grown into LB-broth with Carbenicillin overnight at 37°C under shaking. Plasmid was extracted following the kit (Zymo D4210), and concentration was measured using nanodrop. Plasmids were sequenced by Eurofins to check gRNA integration.

Confocal Imaging

hPSCs were seeded using GD passaging on MG-coated glass bottom dishes (MatTek). The next day, 5μM blebbistatin, 50 nM bafilomycin, or equivalent volume of DMSO was added to the culture media for 24h. Media was aspirated and cells were washed with 1X PBS, and then fixed with 4% Paraformaldehyde for 30 min at 37°C. Cells were washed once and then stored in PBS at 4°C until immunostained. Fixed cells were permeabilized with 0.5% Triton-X100 in PBS for 5 min and then washed in PBST (1X PBS + 0.1% Tween20) for 3 times for 5 minutes each. Cells were blocked with PBS containing 5% donkey serum and 0.1% Tween 20 (blocking buffer). Alexa Fluor 488 conjugated Phalloidin (4U/ml) was added to the blocking buffer and incubated with the cells for 1h in the dark at room temperature. Dishes were washed with 1X PBST 3 times for 5 minutes each, with 1.43 μM DAPI added to the second wash. Cells were stored in 1x PBS while being imaged on Zeiss LSM700 with 63x/1.4 oil objective. Analysis was done using ImageJ with maximum projections of DAPI channel and the middle confocal slice of the Phalloidin labelled F-actin channel of the z-stacks.

CRISPR-Cas9 genome editing of hESCs

H7-hESC colonies were grown and transfected with the plasmid containing HPRT1-gRNA and Cas9 (gRNA cloning protocol) using 600 ng of plasmid with 50 μl optimem and 2 μl lipofectamine stem (Invitrogen). Colony dissection was performed 24h after transfection; edge and center samples were collected and plated into mT with 5 μM blebbistatin in a 96 well MG-coated plate, with each colony piece in its own well. After 24h, media was changed to mT without blebbistatin, with culture continuing for another 7-10 days with mT changed daily. After cells had grown sufficiently, media was aspirated and 30 μl of quick extraction buffer was added to each well and a pipet was used to mix and scrape any

cells from the plate and transfer them into PCR tubes. Samples were then vortexed, spun down, and heated at 65°C for 10 min followed by 95°C for 5 min to extract DNA. After which the concentration was measured on a nanodrop and 50-200 ng of DNA was used with Phusion-Flash mastermix to PCR amplify the DNA sequence around the HPRT1 gRNA target site. The PCR product was run in 1.5% agarose gel with Ethidium Bromide, and gel extracted following the kit (Zymo D4007). Extracted DNA was then sent for sequencing with Eurofins and analyzed with TIDE analysis software (https://tide.nki.nl/) where CRISPR edge samples were compared to the respective centers.

Lentivirus

H7-hESCs at ~80% confluency were clump passaged using GD and seeded into 96-well MG coated wells. The next day, cell counting was done from a well using accutase mediated single cell dissociation. Lentivirus (LV) (Life Technologies Cat # A32060) with viral vector containing P_{U6}-HPRT1(gRNA)-P_{EFS}-GFP was added at multiplicity of infection (MOI) of 10 for each well. LV was added through mT media containing 8 μg/mL polybrene and the plate was centrifuged at 800 G at room temperature for 1h before incubating at 37°C, 5% CO_2 incubator overnight. The next day, media with lentivirus was removed and replaced with normal mT; mT was changed every following day and GFP signal was observed over time.

Quantification and Statistical analysis:

All data presented are mean ± SEM. For statistical analysis between two independent conditions a Student's *t-test* was performed in Microsoft Excel; for more than two

conditions, one-way Anova with Dunnett's multiple comparison post hoc test was performed using GraphPad Prism 9.0 software.

REFERENCES

Anding, A.L., and Baehrecke, E.H. (2017). Cleaning House: Selective Autophagy of Organelles. Dev. Cell *41*, 10–22.

Bhise, N.S., Wahlin, K.J., Zack, D.J., and Green, J.J. (2013). Evaluating the potential of poly(beta-amino ester) nanoparticles for reprogramming human fibroblasts to become induced pluripotent stem cells. Int. J. Nanomedicine *8*, 4641–4658.

Brinkman, E.K., Chen, T., Amendola, M., and Van Steensel, B. (2014). Easy quantitative assessment of genome editing by sequence trace decomposition. Nucleic Acids Res. *42*.

Byrne, S.M., and Church, G.M. (2015). CRISPR-mediated gene targeting of human induced pluripotent stem cells. Curr. Protoc. Stem Cell Biol. *2015*, 5A.8.1-5A.8.22.

Chen, K.G., Mallon, B.S., Hamilton, R.S., Kozhich, O.A., Park, K., Hoeppner, D.J., Robey, P.G., and McKay, R.D.G. (2012). Non-colony type monolayer culture of human embryonic stem cells. Stem Cell Res. *9*, 237–248.

Chen, K.G., Mallon, B.S., McKay, R.D.G., and Robey, P.G. (2014). Human pluripotent stem cell culture: Considerations for maintenance, expansion, and therapeutics. Cell Stem Cell *14*, 13–26.

Das, A., Fischer, R.S., Pan, D., and Waterman, C.M. (2016). YAP nuclear localization in the absence of cell-cell contact is mediated by a filamentous actin-dependent, Myosin

488 IIand Phospho-YAP-independent pathway during extracellular matrix mechanosensing.
489 J. Biol. Chem. *291*, 6096–6110.
490 Ding, Q., Regan, S.N., Xia, Y., Oostrom, L.A., Cowan, C.A., and Musunuru, K. (2013).
491 Enhanced efficiency of human pluripotent stem cell genome editing through replacing
492 TALENs with CRISPRs. Cell Stem Cell *12*, 393–394.
493 Hendel, A., Kildebeck, E.J., Fine, E.J., Clark, J.T., Punjya, N., Sebastiano, V., Bao, G.,
494 and Porteus, M.H. (2014). Quantifying genome-editing outcomes at endogenous loci
495 with SMRT sequencing. Cell Rep. *7*, 293–305.
496 Hendel, A., Bak, R.O., Clark, J.T., Kennedy, A.B., Ryan, D.E., Roy, S., Steinfeld, I.,
497 Lunstad, B.D., Kaiser, R.J., Wilkens, A.B., et al. (2015). Chemically modified guide
498 RNAs enhance CRISPR-Cas genome editing in human primary cells. Nat. Biotechnol.
499 *33*, 985–989.
500 Kroemer, G., Mariño, G., and Levine, B. (2010). Autophagy and the Integrated Stress
501 Response. Mol. Cell *40*, 280–293.
502 Lombardo, A., Genovese, P., Beausejour, C.M., Colleoni, S., Lee, Y.L., Kim, K.A.,
503 Ando, D., Urnov, F.D., Galli, C., Gregory, P.D., et al. (2007). Gene editing in human
504 stem cells using zinc finger nucleases and integrase-defective lentiviral vector delivery.
505 Nat. Biotechnol. *25*, 1298–1306.
506 Martin, R.M., Ikeda, K., Cromer, M.K., Uchida, N., Nishimura, T., Romano, R., Tong,
507 A.J., Lemgart, V.T., Camarena, J., Pavel-Dinu, M., et al. (2019). Highly Efficient and
508 Marker-free Genome Editing of Human Pluripotent Stem Cells by CRISPR-Cas9 RNP
509 and AAV6 Donor-Mediated Homologous Recombination. Cell Stem Cell *24*, 821-828.e5.
510 Mignon, C., Sodoyer, R., and Werle, B. (2015). Antibiotic-free selection in

511 biotherapeutics: Now and forever. Pathogens *4*, 157–181.

512 Närvä, E., Stubb, A., Guzmán, C., Blomqvist, M., Balboa, D., Lerche, M., Saari, M.,

513 Otonkoski, T., and Ivaska, J. (2017). A Strong Contractile Actin Fence and Large

514 Adhesions Direct Human Pluripotent Colony Morphology and Adhesion. Stem Cell

515 Reports *9*, 67–76.

516 Ran, F.A., Hsu, P.D., Wright, J., Agarwala, V., Scott, D.A., and Zhang, F. (2013).

517 Genome engineering using the CRISPR-Cas9 system. Nat. Protoc. *8*, 2281–2308.

518 Rosowski, K.A., Mertz, A.F., Norcross, S., Dufresne, E.R., and Horsley, V. (2015).

519 Edges of human embryonic stem cell colonies display distinct mechanical properties

520 and differentiation potential. Sci. Rep. *5*.

521 Saha, K., and Jaenisch, R. (2009). Technical Challenges in Using Human Induced

522 Pluripotent Stem Cells to Model Disease. Cell Stem Cell *5*, 584–595.

523 Sha, Z., Schnell, H.M., Ruoff, K., and Goldberg, A. (2018). Rapid induction of p62 and

524 GAB ARA PL1 upon proteasome inhibition promotes survival before autophagy

525 activation. J. Cell Biol. *217*, 1757–1776.

526 Sharma, P., Yan, F., Doronina, V.A., Escuin-Ordinas, H., Ryan, M.D., and Brown, J.D.

527 (2012). 2A peptides provide distinct solutions to driving stop-carry on translational

528 recoding. Nucleic Acids Res. *40*, 3143–3151.

529 Sluch, V.M., Chamling, X., Wenger, C., Duan, Y., Rice, D.S., and Zack, D.J. (2018).

530 Highly efficient scarless knock-in of reporter genes into human and mouse pluripotent

531 stem cells via transient antibiotic selection. PLoS One *13*.

532 Steyer, B., Bu, Q., Cory, E., Jiang, K., Duong, S., Sinha, D., Steltzer, S., Gamm, D.,

533 Chang, Q., and Saha, K. (2018). Scarless Genome Editing of Human Pluripotent Stem

534 Cells via Transient Puromycin Selection. Stem Cell Reports *10*, 642–654.

535 Tojkander, S., Gateva, G., and Lappalainen, P. (2012). Actin stress fibers - Assembly,

536 dynamics and biological roles. J. Cell Sci. *125*, 1855–1864.

537 Vandermeulen, G., Marie, C., Scherman, D., and Préat, V. (2011). New generation of

538 plasmid backbones devoid of antibiotic resistance marker for gene therapy trials. Mol.

539 Ther. *19*, 1942–1949.

540 Yang, L., Guell, M., Byrne, S., Yang, J.L., De Los Angeles, A., Mali, P., Aach, J., Kim-

541 Kiselak, C., Briggs, A.W., Rios, X., et al. (2013). Optimization of scarless human stem

542 cell genome editing. Nucleic Acids Res. *41*, 9049–9061.

543 Yen, J., Yin, L., and Cheng, J. (2014). Enhanced non-viral gene delivery to human

544 embryonic stem cells via small molecule-mediated transient alteration of the cell

545 structure. J. Mater. Chem. B *2*, 8098–8105.

546

Figure 1. hESCs selectively get transfected at the colony edges but not center.

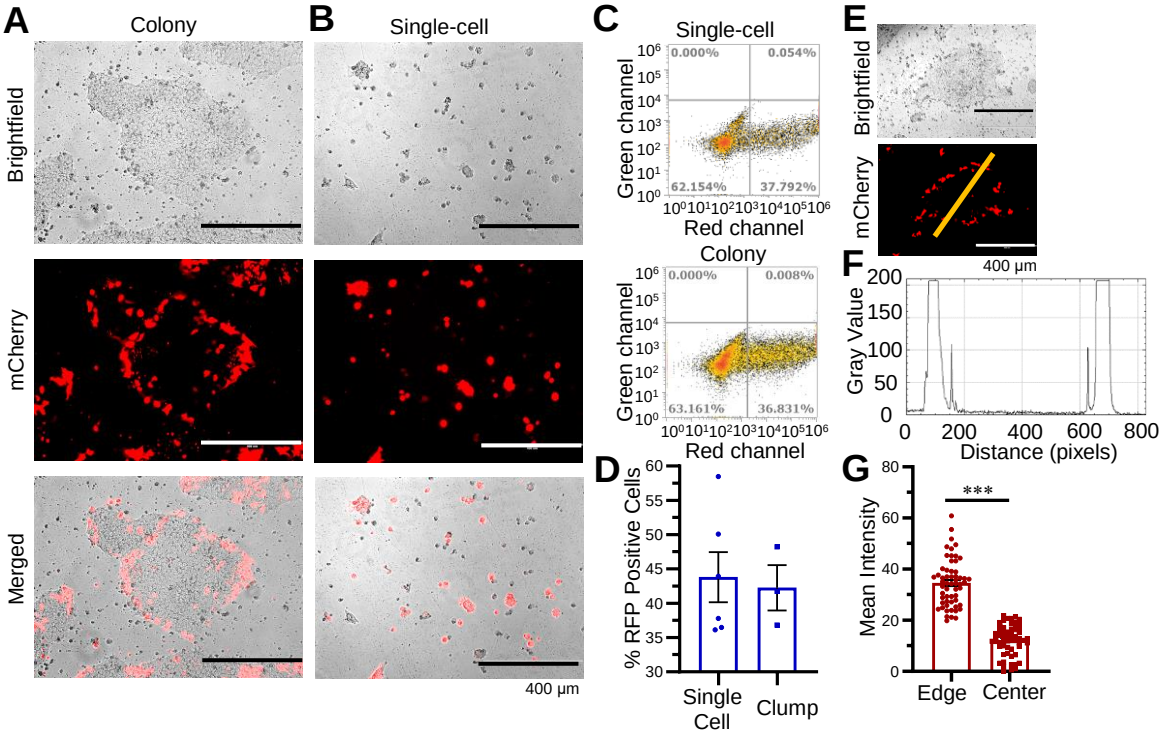

Figure 2. hPSCs at the colony edges are healthier with reduced expression of autophagy genes.

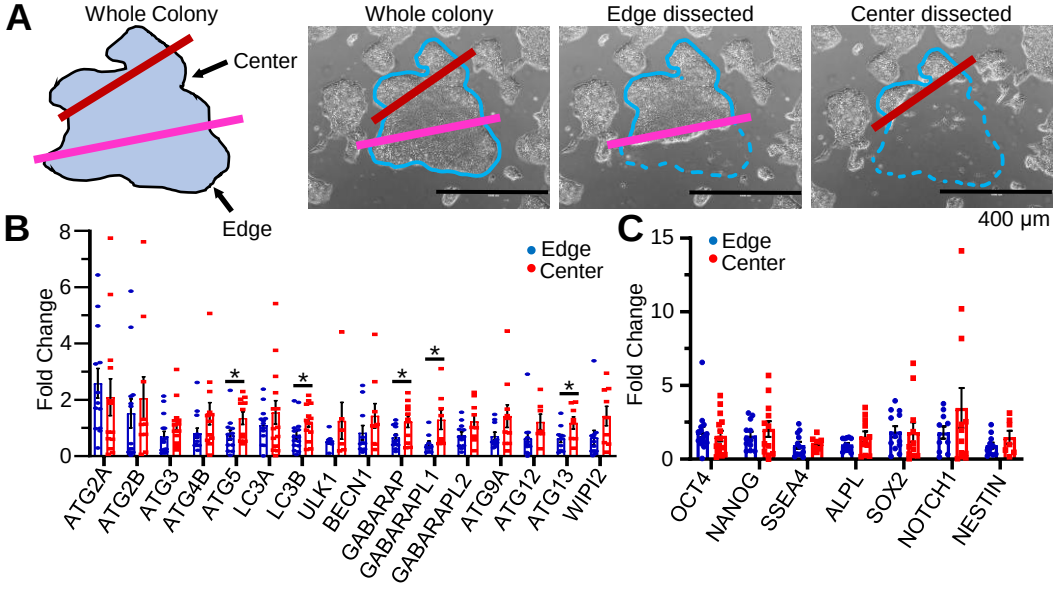

Figure 3. Inhibiting autophagy but not actomyosin contractility decreases transfection efficiency.

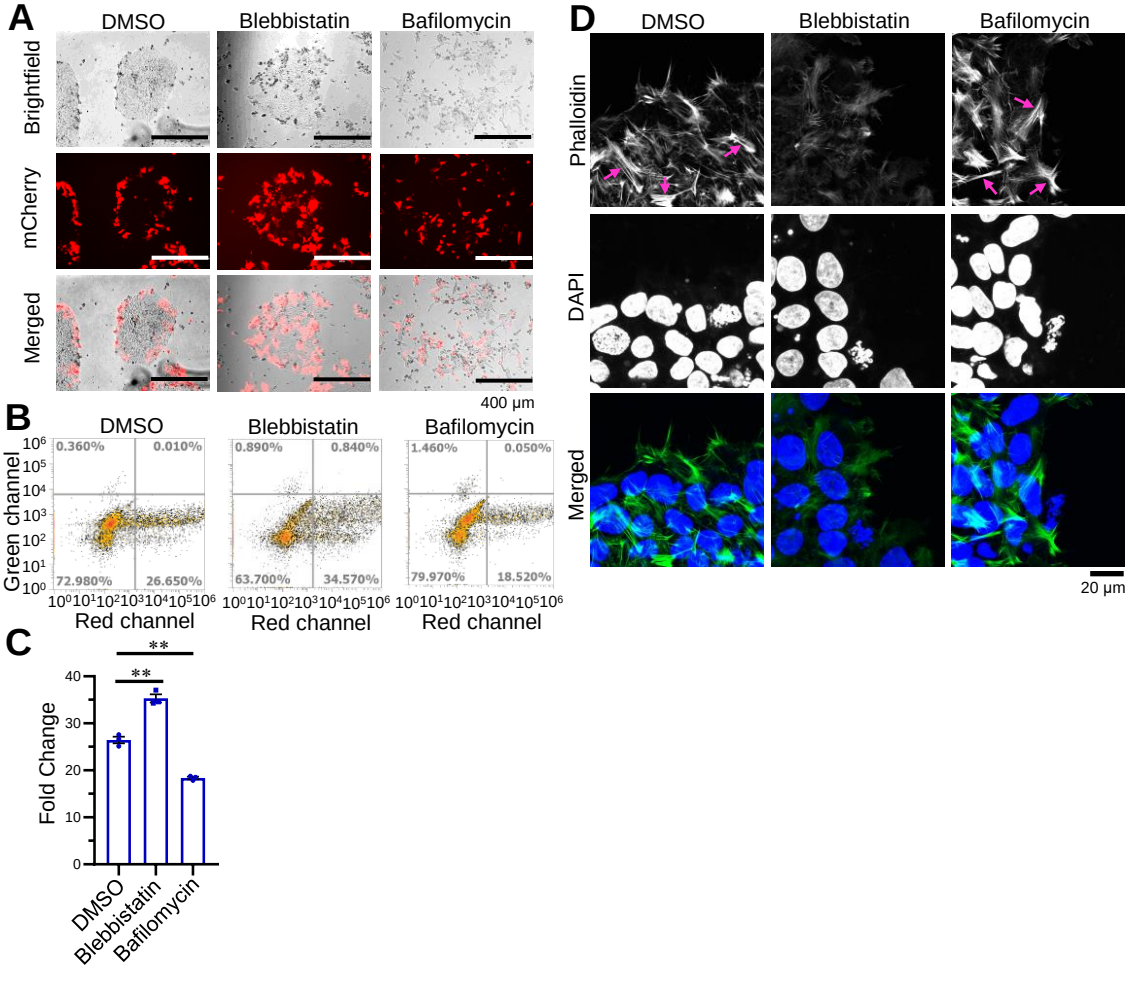

Figure 4. Enhanced CRISPR-Cas9 genome editing at the hPSC colony edges.

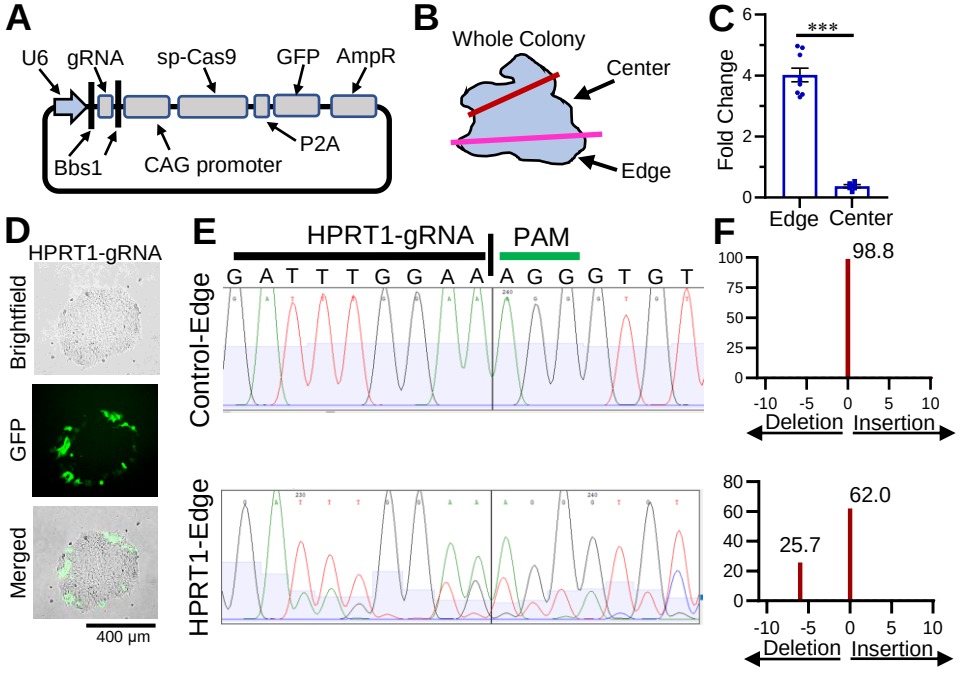

KEY RESOURCES TABLE

REAGENT or RESOURCE	SOURCE	IDENTIFIER
Antibodies		
Alexa Fluor 488 Phalloidin	Invitrogen	Cat# A12379
Bacterial and Virus Strains		
Invitrogen™ One Shot™ TOP10 Chemically Competent *E. coli*	Fisher Scientific	Cat# C404003
Chemicals, Peptides, and Recombinant Proteins		
Matrigel	Corning	Cat# CB40230
Gentle Cell Dissociation Reagent	Stem Cell Technology	Cat# 7174
mTeSR1	Stem Cell Technology	Cat# 85850
mTeSR-Plus	Stem Cell Technololgy	Cat# 5825
Accutase	Sigma	Cat# A6964
Blebbistatin	Sigma	Cat# B0560
Bafilomycin	Sigma	Cat# B1793
DAPI	Molecular Probes	Cat# D1206
DMSO	Sigma	Cat# 276855
Lipofectamine Stem	Invitrogen	Cat# STEM00003
Optimem	Gibco	Cat# 31985070
Parafomaldehyde 16% solution, EM grade	Electron Microscopy Sciences	Cat# 15710
Triton-X-100	Sigma	Cat# T8787
Donkey Serum	Sigma	Cat# D9663
Tween-20	Sigma	Cat# P9416
Polybrene	Sigma	Cat# TR-1003-G
Bbs1-HF	New England BioLabs	Cat# R3539S
Cutsmart Buffer	New England BioLabs	Cat# B7204S
T4 DNA Ligase Reaction Buffer	New England BioLabs	Cat# B0202S
T4 Polynucleotide Kinase (PNK)	New England BioLabs	Cat# M0201S
Quick Ligation Buffer	New England BioLabs	Cat# B2200
Quick Ligase	New England BioLabs	Cat# M2200S
SOC media	Fisher Scientific	Cat# BP974010X5
Carbenicillin	Sigma	Cat# C1389
LB Broth (Miller)	Sigma	Cat# L3522
LB broth with agar (Miller)	Sigma	Cat# L3147
Quick Extraction Buffer	Epicentre	Cat# QE09050
Phusion Flash Mastermix	Fisher Scientific	Cat# F548L
Agarose	Sigma	Cat# A9539
Ethidium Bromide	Sigma	Cat# E1510
Critical Commercial Assays		
RNeasy Mini Kit	Qiagen	Cat# 74104
5x all-in-one RT MasterMix (with AccuRTGenomic DNA Removal kit)	applied biological materials	Cat# G492
BrightGreen 2x qPCR MasterMix-Low ROX	applied biological materials	Cat# MasterMix-LR
ZymoPURE™ Plasmid Miniprep Kit	Zymo	Cat# D4210
Zymoclean Gel DNA Recovery Kit	Zymo	Cat# D4007

Experimental Models: Cell Lines		
H7-hESCs, H9-hESCs	WiCell; Sluch et al., 2018	
EP1-iPSCs	Bhise et al., 2013	
Oligonucleotides		
HPRT1-gRNA-Forward	ThermoFisher website; alterations following Ran et al., 2013	CACCGATTATGCT GAGGATTTGGAA
HPRT1-gRNA-Reverse	ThermoFisher website; alterations following Ran et al., 2013	AAACTTCCAAATC CTCAGCATAATC
gRNA plasmid sequencing		CGCCAGCAACGC GGCCTTTTTACGG
HPRT1-PCR-Forward; sequencing	ThermoFisher website	TACACGTGTGAAC CAACCCG
HPRT1-PCR-Reverse	ThermoFisher website	GTAAGGCCCTCCT CTTTTATTT
Primers for qPCR	Supplemental Table S1	
Recombinant DNA		
pCAG-mCherry plasmid	Addgene	Cat# 108685
pCAG-SpCas9-P2A-GFP-U6-gRNA	Addgene	Cat# 79144
pCAG-SpCas9-P2A-GFP-U6-HPRT1	This paper	N/A
LentiArray™ CRISPR Positive Control Lentivirus, human HPRT, with GFP (P_{U6}-HPRT1-P_{EFS}-GFP)	ThermoFisher (Life Technologies)	Cat# A32060
Software and Algorithms		
ImageJ	NIH	
Attune NxT Software	ThermoFisher	
Prism version 9	GraphPad	
Zen Microscope Software	Zeiss	
Genescript	https://www.genscript.com/	
Primer3	https://primer3.ut.ee/	
PrimerBank	https://pga.mgh.harvard.edu/primerbank/	
TIDE analysis software	https://tide.nki.nl/	